

Coulomb exchange functional with generalized gradient approximation for self-consistent Skyrme Hartree-Fock calculations

Tomoya Naito (内藤智也),^{1,2} Xavier Roca-Maza,^{3,4}
Gianluca Colò,^{3,4} and Haozhao Liang (梁豪兆)^{2,1,*}

¹*Department of Physics, Graduate School of Science,
The University of Tokyo, Tokyo 113-0033, Japan*

²*RIKEN Nishina Center, Wako 351-0198, Japan*

³*Dipartimento di Fisica, Università degli Studi di Milano,
Via Celoria 16, 20133 Milano, Italy*

⁴*INFN, Sezione di Milano, Via Celoria 16, 20133 Milano, Italy*

(Dated: January 25, 2020; 0_proton_scf)

Abstract

We perform the self-consistent Skyrme Hartree-Fock calculation with the Coulomb exchange functional in the form of generalized gradient approximation (GGA). It is found that the Perdew-Burke-Ernzerhof GGA (PBE-GGA) Coulomb exchange functional is able to reproduce the exact-Fock energy for the nuclei in a large region of the nuclear chart with one adjustable parameter. The remaining error of Coulomb exchange energy by the GGA with respect to the exact-Fock energy dominantly comes from the functional-driven error.

* haozhao.liang@riken.jp

I. INTRODUCTION

Atomic nuclei are composed of protons and neutrons that interact with each other through the nuclear and electromagnetic forces. Since it is much stronger than the electromagnetic one, the nuclear force mainly determines the properties of atomic nuclei. Nevertheless, in specific studies it is important to evaluate the electromagnetic contribution to the properties of atomic nuclei, for example, for the mass difference of mirror nuclei [1], the energy of the isobaric analog state [2–4], the isospin symmetry breaking of nuclear force [5], and the superallowed Fermi β decay [6, 7]. Since the static electromagnetic force is well known and mainly associated with the Coulomb contribution, it is in principle possible to evaluate the contribution of electromagnetic force for such phenomena with high accuracy.

The exchange term of two-body interaction is characteristic for Fermionic systems. In nuclear physics, the Coulomb exchange term is calculated in the exact form in some studies, including the non-relativistic [8–12] and relativistic Hartree-Fock calculations [13, 14]. However, due to its numerical costs, the Coulomb exchange energy density functional is usually treated as the local density approximation (LDA), i.e., the Hartree-Fock-Slater approximation [15, 16] and its relativistic version [17–19], or even neglected [20, 21].

Recently it has been shown that Coulomb energy density functionals of the generalized gradient approximation (GGA) give almost the same accuracy as the exact-Fock energy [22] by using the experimental charge density distribution as inputs of the functional. As a step further, the corresponding self-consistent calculation in the scheme of the Skyrme Hartree-Fock theory and quantitative discussions are highly desired. Self-consistent calculation with the GGA Coulomb exchange functional has an advantage for the numerical cost since the numerical cost of the self-consistent calculation with the GGA Coulomb exchange functional is $O(N^3)$, while that with the exact-Fock term is $O(N^4)$ [23].

One of the relevant topics is a free parameter μ in the Perdew-Burke-Ernzerhof GGA (PBE-GGA) Coulomb exchange functional, which will be defined in Sec. II. As we discuss in detail below, the form of the PBE-GGA functional was determined in order to satisfy several physical conditions [24, 25]. Two different values of μ have been widely used in the studies of atoms [25] and solids [26], respectively. In this paper, we carry out the self-consistent Skyrme Hartree-Fock calculation by using the PBE-GGA functional instead of the exact-Fock. Therefore, the optimal value of μ and its applicability will be discussed in

detail.

This paper is organized in the following way: First, the theoretical framework and general discussion for the PBE-GGA is given in Sec. II. Second, the calculation setup is explained in Sec. III. The systematic calculations and discussion are shown in Subsec. IV A, and detailed analysis for ^{208}Pb is shown in Subsec. IV B. Finally, the conclusions and perspectives of this paper are shown in Sec. V. The potential form and rearrangement term for the GGA Coulomb exchange functional are shown in Appendix.

II. THEORETICAL FRAMEWORK

The LDA Coulomb exchange functional [15, 16] is well known as the Hartree-Fock-Slater approximation, which reads

$$E_{\text{Cx}}^{\text{LDA}}[\rho_{\text{ch}}] = -\frac{3}{4} \frac{e^2}{4\pi\epsilon_0} \left(\frac{3}{\pi}\right)^{1/3} \int [\rho_{\text{ch}}(\mathbf{r})]^{4/3} d\mathbf{r}, \quad (1)$$

where ρ_{ch} is the charge density distribution. In order to go beyond the LDA, the GGA Coulomb exchange functionals [25–27] have been proposed as

$$E_{\text{Cx}}^{\text{PBE}}[\rho_{\text{ch}}] = -\frac{3}{4} \frac{e^2}{4\pi\epsilon_0} \left(\frac{3}{\pi}\right)^{1/3} \int [\rho_{\text{ch}}(\mathbf{r})]^{4/3} F(s(\mathbf{r})) d\mathbf{r}, \quad (2)$$

where F is the enhancement factor due to the density gradient. Here, s denotes the dimensionless density gradient

$$s = \frac{|\nabla\rho_{\text{ch}}|}{2k_{\text{F}}\rho_{\text{ch}}}, \quad k_{\text{F}} = (3\pi^2\rho_{\text{ch}})^{1/3}. \quad (3)$$

In particular, the enhancement factor F in the PBE-GGA Coulomb exchange functional is assumed to be [25]

$$F(s) = 1 + \kappa - \frac{\kappa}{1 + \mu s^2/\kappa}, \quad (4)$$

in order to satisfy some physical conditions shown below [24]. Accordingly, the parameters κ and μ are determined to satisfy the same conditions.

Firstly, in the uniform density distribution, i.e., $s = 0$, the PBE-GGA Coulomb exchange functional should represent the LDA one. Thus,

$$F(0) = 1 \quad (5)$$

is trivially required.

Secondly, the Coulomb exchange functional should satisfy the Lieb-Oxford bound [28], that is an analytical inequality

$$E_{\text{Cx}}[\rho_{\text{ch}}] \geq -1.679 \int [\rho_{\text{ch}}(\mathbf{r})]^{4/3} d\mathbf{r}, \quad (6)$$

which is derived from the Hölder inequality in mathematics [29]. In order to satisfy this condition, the parameter κ is determined as $\kappa = 0.804$ for any value of μ .

Thirdly, the PBE-GGA Coulomb exchange functional should also satisfy the uniform scaling [30]

$$E_{\text{Cx}}[\zeta^3 \rho_{\text{ch}}(\zeta \mathbf{r})] = \zeta E_{\text{Cx}}[\rho_{\text{ch}}(\mathbf{r})] \quad (7)$$

for any ζ in order to satisfy the condition of the exchange hole

$$\int P_{\parallel}(\mathbf{r}, \mathbf{r} + \mathbf{u}) d\mathbf{u} = -1 \quad (8)$$

for all \mathbf{r} , where

$$P_{\parallel}(\mathbf{r}_1, \mathbf{r}_2) = \frac{1}{N(N-1)} \sum_{\sigma=\uparrow, \downarrow} \rho^{\sigma}(\mathbf{r}_1) [\rho^{\sigma}(\mathbf{r}_2) + \rho_{\text{x}}^{\sigma}(\mathbf{r}_1, \mathbf{r}_2)], \quad (9)$$

$$\rho^{\sigma}(\mathbf{r}) = \sum_j |\psi_{j\sigma}(\mathbf{r})|^2, \quad (10)$$

$$\rho_{\text{x}}^{\sigma}(\mathbf{r}_1, \mathbf{r}_2) = -\frac{|\sum_j \psi_{j\sigma}^*(\mathbf{r}_1) \psi_{j\sigma}(\mathbf{r}_2)|}{\rho^{\sigma}(\mathbf{r}_1)}. \quad (11)$$

Here, $\psi_{j\sigma}$ is the Kohn-Sham single-particle orbital for the j -th occupied state, σ is the spin coordinate, and \uparrow and \downarrow represent the spin-up and spin-down states, respectively.

Finally, at the slowly varying limit, i.e., $s \simeq 0$, in order to recover the LDA response function, the PBE-GGA Coulomb functional represents the linear response of the homogeneous electron gas as [24]

$$\lim_{s \rightarrow 0} F(s) = 1 + \mu s^2, \quad (12)$$

with $\mu = 0.21951$. This μ can be understood as a coefficient in a response function theory since it multiplies a term proportional to the square of the gradient of the charge density [24, 31].

Combining Eqs. (5), (6), (7), and (12), the PBE-GGA enhancement factor F is determined as Eq. (4). This discussion can be applied to proton systems if protons are assumed to be point particles, since protons and electrons share common properties from the point

of view of electromagnetic interaction. However, the value of μ is still under discussion. The enhancement factor of the PBEsol-GGA Coulomb exchange functional [26] is also determined to satisfy the same conditions as the PBE-GGA one, while at the $s \rightarrow 0$ limit $\mu = 0.1235$ instead [31], and as a result, it is empirically known that the PBEsol-GGA Coulomb functional reproduce electron structure of solids better than the PBE-GGA one. Therefore, the coefficient μ can be considered as a free parameter, while the coefficient κ is fixed.

III. CALCULATION SETUP

The LDA and PBE-GGA Coulomb exchange functionals are applied to the self-consistent Skyrme Hartree-Fock calculation [32], while for the nuclear part of EDF the SAMi functional [33] is used. Here, note that no refit of the nuclear part of EDF is needed due to the use of the PBE-GGA functional for the Coulomb exchange term since this term produces at most a difference of 1 MeV in the total binding energy with respect to LDA. Therefore, the difference does not deteriorate the quality of SAMi in the description of bulk properties such as binding energies or charge radii. In this paper protons are treated as point particle as in the usual treatment, i.e. $\rho_{\text{ch}} = \rho_p$, where ρ_{ch} and ρ_p are the ground-state charge and proton density distributions, respectively. Since the PBE-GGA Coulomb exchange functional is written in terms of the density, the form factor of nucleon can be considered in the self-consistent steps, and this finite-size effect will be considered as a future study.

For the numerical calculation, the `skyrme_rpa` code [34] is used. In this code, spherical symmetry is assumed and a box of 15 fm with a mesh of 0.1 fm is used. Here, there is no need of pairing correlations for the doubly-magic nuclei, while the pairing correlations are neglected in open-shell nuclei. Although the pairing correlations might be important for a detailed comparison to experiment, this is not the aim of the present study. The purpose here is to understand if our new local Coulomb functional can provide a satisfactory description of the exact Coulomb exchange energy in the Skyrme Hartree-Fock calculations for finite nuclei when calculated within the same conditions.

In the Skyrme Hartree-Fock calculation, the total energy can be written in two ways: One way is

$$E_{\text{gs}} = T_0 + E_{\text{nucl}}[\rho_p, \rho_n] + E_{\text{Cd}}[\rho_{\text{ch}}] + E_{\text{Cx}}[\rho_{\text{ch}}], \quad (13)$$

where ρ_n is the ground-state neutron density distribution, T_0 is the kinetic energy, and E_{nucl} , E_{Cd} , and E_{Cx} are nuclear, Coulomb direct, and Coulomb exchange functionals, respectively.

The other way is

$$E_{\text{gs}} = \frac{1}{2} \sum_j (\varepsilon_j + \tau_j) + E_{\text{rea}}, \quad (14)$$

where ε_j and τ_j are the single-particle energy and single-particle kinetic energy, respectively, and E_{rea} is the energy of rearrangement term. In all of the present calculations, we find $(E_{\text{tot}}^2 - E_{\text{tot}}^1) / E_{\text{tot}}^1$ is of the order of 10^{-4} , where E_{tot}^1 and E_{tot}^2 are the total energies calculated by Eqs. (13) and (14), respectively. Hence, the numerical accuracy of the presented results is of the order of 0.01 %, well below the average model accuracy in the description of nuclear ground-state energies [35].

IV. RESULTS AND DISCUSSION

A. Systematic calculations

The Coulomb exchange energies E_{Cx} for the doubly-magic nuclei calculated in the LDA and PBE-GGA Coulomb exchange functionals are shown in Table I. For comparison, the exact-Fock energies are also calculated, where the exact-Fock calculation is carried out by the first-order perturbation theory [12]. This is assumed to be accurate enough for our purpose of discussion. In order to see the difference between the LDA and PBE-GGA clearly, the deviation of the Coulomb exchange energy E_{Cx} in the PBE-GGA from that in the LDA,

$$\Delta E_{\text{Cx}} = \frac{E_{\text{Cx}} - E_{\text{Cx}}^{\text{LDA}}}{E_{\text{Cx}}}, \quad (15)$$

is also shown as a function of mass number A in Fig. 1. Results calculated from the exact-Fock and PBE-GGA are shown with squares and down-triangles, respectively. It is seen that in the light-mass region ΔE_{Cx} is more than 10 %, while in the medium-heavy- and heavy-mass regions ΔE_{Cx} decreases gradually with A . This is because the ratio of the surface region in the light nuclei is larger than that in the medium-heavy or heavy nuclei as discussed in Ref. [22]. From light nuclei to heavy nuclei, the PBE-GGA results show similar behavior as the exact-Fock results.

However, it is also seen that absolute values of the PBE-GGA Coulomb exchange energy are a little smaller than those of the exact-Fock energy systematically. In order to improve

it, the free parameter of the PBE-GGA Coulomb exchange functional, μ , is multiplied by a factor λ . According to Eq. (12), larger λ gives larger enhancement factor F . The Coulomb exchange energies E_{C_x} calculated with $\lambda = 1.25$ and 1.50 are shown in Table I, while the corresponding deviations ΔE_{C_x} in Eq. (15) are shown with circles and up-triangles, respectively, in Fig. 1. It is found that in the light-mass region in order to reproduce the exact-Fock result $\lambda = 1.50$ or larger is required, and in the medium-heavy- and heavy-mass regions $\lambda = 1.25$ reproduces the exact-Fock results well. The PBE-GGA with $\lambda = 1.00$ reproduces the exact-Fock result for the super-heavy nucleus $^{310}126$. The behavior in Fig. 1 has also been calculated for other Skyrme functionals (e.g. SLy5) showing a negligible dependence on the used parametrization.

By comparing the results of ^{40}Ca and ^{48}Ca , one may consider that the factor λ has an isospin $(N - Z)/A$ dependence. In order to see the difference between the LDA to PBE-GGA in isotopic chains, ΔE_{C_x} for the O, Ca, and Sn isotopes are shown as a function of A in Fig. 2. As shown in Fig. 2, the PBE-GGA with $\lambda = 1.50$ reproduces the exact-Fock results for all O isotopes, and that with $\lambda = 1.25$ reproduces the exact-Fock results for all Sn isotopes. For Ca isotope, $\lambda = 1.50$ reproduces well in ^{40}Ca , while $\lambda = 1.25$ reproduces well in ^{48}Ca . Nevertheless, the Ca isotopes have some open questions, for example, the charge radius of ^{48}Ca is smaller than that of ^{40}Ca [36], whereas nucleus with the larger mass number has larger charge radius in usual isotopes. Hence, the behavior of λ in Ca isotopes is an open problem.

Furthermore, in light nuclei, density properties are more sensitive to the shell structure, and thus λ may be sensitive to A , Z , etc. In contrast, in medium-heavy and heavy nuclei density properties are less sensitive to the shell structure. Hence, λ is somehow universal for a large region of nuclear chart.

As a conclusion, λ does not have an obvious isospin dependence, and $\lambda = 1.25$ reproduces the exact-Fock calculation well in general. Here, note that the PBE-GGA Coulomb potential is the local potential and thus the numerical cost of the self-consistent calculation is $O(N^3)$, while the exact-Fock Coulomb potential is the non-local potential and thus the numerical cost is $O(N^4)$. Hence, the self-consistent calculation of the PBE-GGA functional with $\lambda = 1.25$ is lower numerical cost than and as almost the same accuracy as that of the exact-Fock calculation.

Before ending this subsection, let us pay more attention to the idea of the exchange

TABLE I. Coulomb exchange energies E_{C_x} for the doubly-magic and semi-magic nuclei calculated with the LDA, PBE-GGA Coulomb exchange functionals, and the exact-Fock. All units are in MeV. For the nuclear part of EDF the SAMi functional [33] is used.

Nucleus	LDA	Exact-Fock	PBE-GGA ($\lambda = 1.00$)	PBE-GGA ($\lambda = 1.25$)	PBE-GGA ($\lambda = 1.50$)
^4He	-0.627	-0.732	-0.701	-0.712	-0.722
^{14}O	-2.866	-3.098	-3.051	-3.082	-3.109
^{16}O	-2.854	-3.088	-3.038	-3.067	-3.094
^{24}O	-2.770	-2.999	-2.946	-2.974	-2.999
^{40}Ca	-7.558	-7.980	-7.879	-7.933	-7.982
^{48}Ca	-7.458	-7.812	-7.774	-7.826	-7.873
^{100}Sn	-19.768	-20.429	-20.347	-20.446	-20.537
^{124}Sn	-19.001	-19.664	-19.558	-19.652	-19.738
^{132}Sn	-18.804	-19.446	-19.359	-19.452	-19.537
^{162}Sn	-17.873	-18.484	-18.398	-18.486	-18.566
^{208}Pb	-31.265	-32.090	-32.013	-32.140	-32.256
$^{310}_{126}$	-48.304	-49.305	-49.266	-49.432	-49.585

functional. In the DFT, ideally, the total Coulomb energy, i.e., the sum of the Coulomb direct, exchange, and correlation energies, has physical meaning instead of each contribution to the energy separately. However, since the Coulomb correlation EDFs are not considered in nuclear physics, the Coulomb exchange EDF discussed here is so far required to reproduce the exact-Fock energy. In contrast, in electron systems, the Coulomb exchange EDF is not supposed to reproduce such an exact-Fock energy. Instead, the exchange and correlation EDFs together aim to reproduce the total energy. Therefore, the roles of the exchange EDF are slightly different from each other. As a result, the value of λ is different from one, yet expected to be of the same order.

B. Detail analysis for ^{208}Pb

In order to understand in more detail, the ground-state properties of ^{208}Pb influenced by the Coulomb interaction will be discussed. In this subsection, $\lambda = 1.25$ is used for the

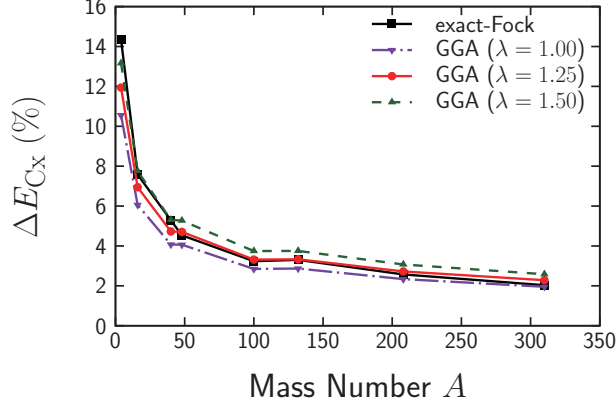


FIG. 1. The deviation of the Coulomb exchange energy E_{C_x} in the PBE-GGA from that in the LDA, ΔE_{C_x} , as a function of A for doubly-magic nuclei. For the nuclear part of EDF the SAMi functional [33] is used. Results calculated from the PBE-GGA with $\lambda = 1.00$, 1.25 , and 1.50 are shown with down-triangles, circles, and up-triangles, respectively. For comparison, the exact-Fock results are shown with squares.

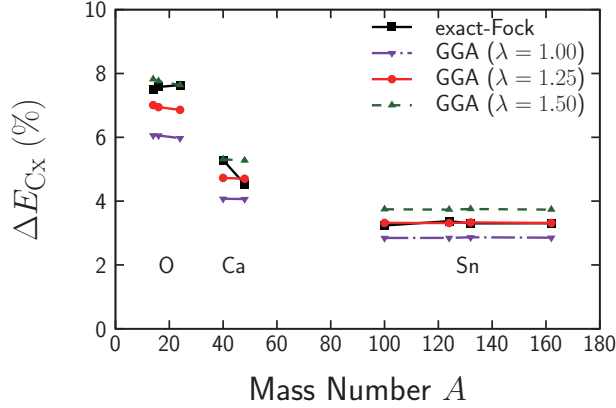


FIG. 2. The same as Fig. 1 but for the O, Ca, and Sn isotopes.

PBE-GGA Coulomb exchange functional.

The LDA and PBE-GGA Coulomb exchange potentials V_{C_x} are shown as a function of r in long-dashed and solid lines, respectively, in Fig. 3(a). In order to see clearly the difference between results calculated by the PBE-GGA Coulomb exchange functional and that by LDA one, the deviation of the PBE-GGA and LDA Coulomb exchange potential

$$\Delta V_{C_x} = \frac{V_{C_x}^{\text{GGA}} - V_{C_x}^{\text{LDA}}}{V_{C_x}^{\text{GGA}}} \quad (16)$$

and the same but for the total Coulomb potential, ΔV_C , are shown in Figs. 3(b) and (c), respectively. It is seen that the deviation between the PBE-GGA and LDA Coulomb exchange

energy is profound, especially -30% in the surface region and 40% in the tail region. The dip in the surface region is because of the derivative of ρ_p , while the asymptotic behavior in the tail region is due to saturation of the enhancement factor F as s increases. However, the Coulomb exchange potential is quite weak compared with the Coulomb direct potential. Thus, though the deviation is non-negligible for Coulomb exchange potential, that for the total Coulomb potential is less than 0.5% .

The proton and neutron density distribution ρ_p and ρ_n for ^{208}Pb are shown as a function of r in Figs. 4(a) and 5(a), respectively. The deviation between the density calculated by the PBE-GGA Coulomb exchange functional from that by the LDA one,

$$\Delta\rho_\tau = \frac{\rho_\tau^{\text{GGA}} - \rho_\tau^{\text{LDA}}}{\rho_\tau^{\text{GGA}}} \quad (\tau = p, n), \quad (17)$$

are shown as a function of r in Figs. 4(b) and 5(b), respectively. Since the Coulomb potential V_C affects proton single-particle orbitals and thus density ρ_p directly, the absolute value of $\Delta\rho_p$ is the same order as ΔV_C . Because the Coulomb functional does not affect the neutron density directly but in the self-consistent step, the absolute value of $\Delta\rho_n$ is one order of magnitude smaller than $\Delta\rho_p$. Even though they are tiny, both $\Delta\rho_p$ and $\Delta\rho_n$ are negative in the surface region, as the PBE-GGA Coulomb potential is larger than the LDA one there. Moreover, since the LDA and PBE-GGA Coulomb exchange functionals give very similar the proton densities ρ_p , the difference of the two Coulomb exchange potential ΔV_{C_x} comes from the enhancement factor instead of the difference of the density.

The single-particle energies ε_j for protons in ^{208}Pb calculated from the LDA and PBE-GGA Coulomb exchange functionals are shown in Table II. Those from the exact-Fock [12] are also shown. Since the Coulomb potential changes quite a little as shown in Fig. 3(c), the single-particle energies also change quite a little. The differences in ε_j calculated by the LDA between those by the PBE-GGA are less than 10 keV , while the differences between those by the LDA and those by the exact-Fock are more than 100 keV . Even though the PBE-GGA Coulomb exchange functional does not change the single-particle energies ε_j , the exchange Coulomb energy E_{C_x} in the PBE-GGA is almost the same as the exact-Fock energy. In order to understand the reason, the exchange Coulomb energy E_{C_x} , the total energy per particle E_{tot}/A , the sum of the single-particle energies and kinetic energies par particle $\sum_j (\varepsilon_j + \tau_j)/2A$, and the energy of rearrangement term par particle E_{rea}/A for ^{208}Pb are shown in Table III, where the total energy is calculated as Eq. (14). It is seen that E_{rea}/A

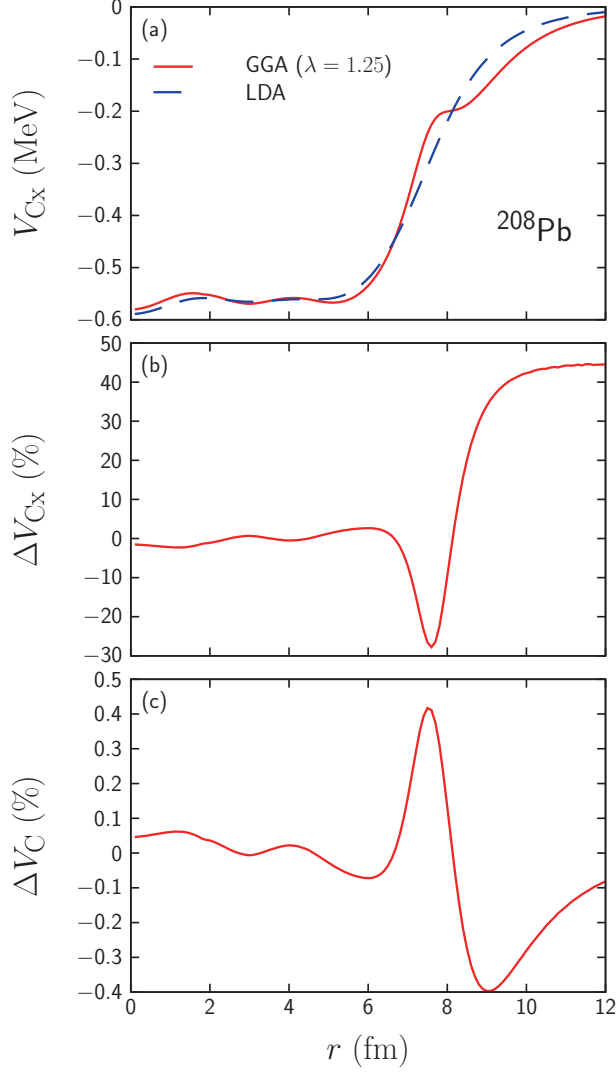


FIG. 3. (a) The LDA (long-dashed line) and PBE-GGA (solid line) Coulomb exchange potentials V_{C_x} as a function of r . (b) The deviation of the PBE-GGA and LDA Coulomb exchange potential ΔV_{C_x} as a function of r . (c) The same as (b) but for the total Coulomb potential ΔV_C .

of the PBE-GGA changes from that of the LDA (0.006 MeV/A), while $\sum_j (\varepsilon_j + \tau_j)/2A$ and E_{rea}/A of the exact-Fock change from those of the LDA (0.054 MeV/A and -0.050 MeV/A, respectively). As a result, the PBE-GGA exchange Coulomb energy is almost the same as the exact-Fock energy (-32.140 MeV).

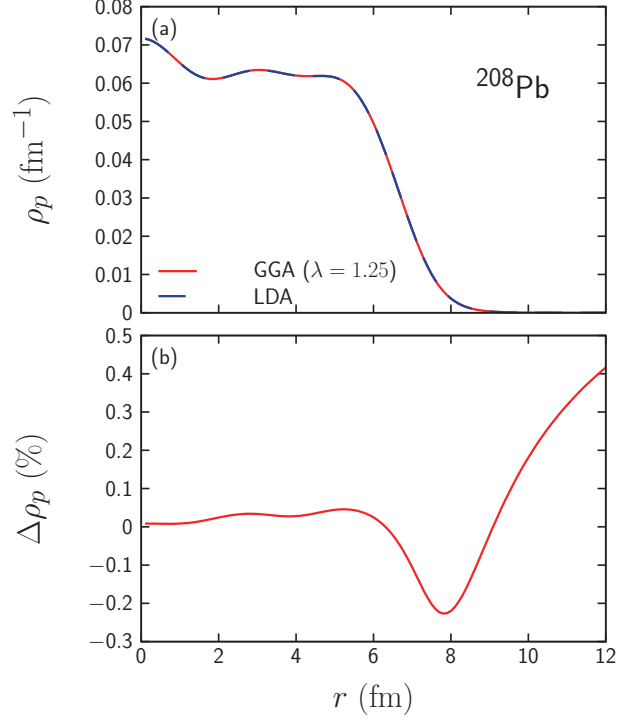


FIG. 4. (a) Proton density distribution ρ_p for ^{208}Pb as a function of r , where the results calculated from the LDA and PBE-GGA are shown in long-dashed and solid lines, respectively. (b) Deviation of the density in PBE-GGA from that in LDA, $\Delta\rho_p$, as a function of r .

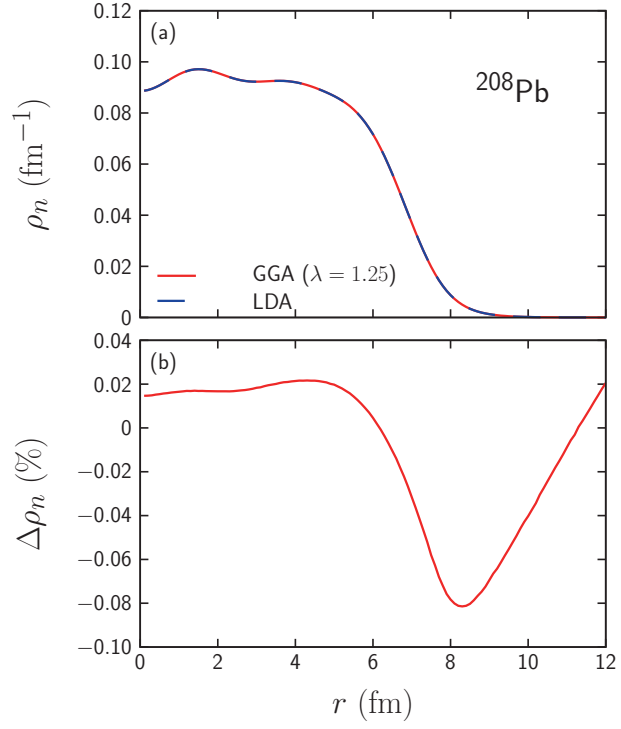


FIG. 5. The same as Fig. 4 but for neutron density distribution ρ_n and deviation $\Delta\rho_n$.

TABLE II. Single-particle energies for protons in ^{208}Pb calculated from the LDA and PBE-GGA Coulomb exchange functionals. Those from the exact-Fock calculation [12] are also shown. All units are in MeV.

Orbital	Exact-Fock [12]	LDA	GGA ($\lambda = 1.25$)
$1s_{1/2}$	-45.501	-44.980	-44.983
$1p_{3/2}$	-39.863	-39.387	-39.390
$1p_{1/2}$	-39.574	-39.107	-39.111
$1d_{5/2}$	-32.903	-32.482	-32.485
$1d_{3/2}$	-32.209	-31.815	-31.817
$2s_{1/2}$	-28.899	-28.509	-28.507
$1f_{7/2}$	-25.045	-24.692	-24.693
$1f_{5/2}$	-23.648	-23.353	-23.353
$2p_{3/2}$	-19.702	-19.411	-19.406
$2p_{1/2}$	-18.906	-18.626	-18.621
$1g_{9/2}$	-16.605	-16.338	-16.336
$1g_{7/2}$	-14.175	-14.019	-14.017
$2d_{5/2}$	-10.411	-10.255	-10.246
$2d_{3/2}$	-8.897	-8.846	-8.837
$3s_{1/2}$	-7.813	-7.673	-7.660
$1h_{11/2}$	-7.802	-7.663	-7.658

TABLE III. Exchange Coulomb energy E_{C_x} , the total energy per particle E_{tot}/A , the sum of the single-particle energies and kinetic energies per particle $\sum_j (\varepsilon_j + \tau_j)/2A$, and the energy of rearrangement term per particle E_{rea}/A for ^{208}Pb . All units are in MeV.

	Exact-Fock	LDA	GGA ($\lambda = 1.25$)
E_{C_x}	-32.090	-31.265	-32.140
E_{tot}/A	-7.872	-7.868	-7.873
$\sum_j (\varepsilon_j + \tau_j)/2A$	-2.225	-2.171	-2.169
E_{rea}/A	-5.647	-5.697	-5.703

V. CONCLUSIONS AND PERSPECTIVES

In this paper, we applied the PBE-GGA Coulomb exchange functional for the self-consistent Skyrme Hartree-Fock calculations for atomic nuclei. In order to reproduce the exact-Fock energy, one of the PBE-GGA parameters μ is changed to $\lambda\mu$. It is found that $\lambda = 1.25$ is the most suitable value for nuclei in a large region of the nuclear chart, and λ does not have an obvious isospin dependence, though there are some open questions for the behavior of the Ca isotopes and for the suitable values for the light- or super-heavy nuclei. It should be emphasized that the numerical cost of the self-consistent calculation with the PBE-GGA exchange functional is $O(N^3)$, whereas that with the exact-Fock is $O(N^4)$.

For the Coulomb exchange energy, it is found that the deviation between the PBE-GGA and the LDA results, ΔE_{C_x} , ranges from around 12 % in ${}^4\text{He}$ to 2 % in ${}^{310}126$. This behavior is similar to ΔE_{C_x} for the exact-Fock. In contrast, it is found that the proton and neutron density distributions and the single-particle energies calculated by the PBE-GGA give almost the same results to those by the LDA, since the Coulomb potential changes quite a little from the LDA to the PBE-GGA. It has been shown that the Coulomb exchange energy in the PBE-GGA reproduces to the Fock energy due to the energy of rearrangement term E_{rea} , not only for ${}^{208}\text{Pb}$ but also for the other nuclei, although we do not show the details explicitly.

It is known that the error of the total Coulomb energy can be separable into two parts: the density-driven error and functional-driven error [37]. The latter comes from the difference between “exact” functional $E[\rho_{\text{gs}}]$ and “approximated” functional $\tilde{E}[\rho_{\text{gs}}]$, and the former is the remaining part and comes from the difference between the exact ground-state density ρ_{gs} and the calculated ground-state density $\tilde{\rho}_{\text{gs}}$. For the Coulomb exchange functional, between the LDA and the PBE-GGA, the calculated ground-state densities are almost the same to each other, and here the exact-Fock energy is calculated by the first-order perturbation theory. Thus, the difference between the PBE-GGA energy and exact-Fock one dominantly comes from the functional-driven error.

The finite-size effect of protons is an interesting topic. Since electrons are elementary particles and do not have a finite radius, charge distribution and electron distribution are identical to each other in electron systems. In contrast, since protons have a finite radius [38], charge distribution ρ_{ch} and proton distribution ρ_p are different to each other. Even

though commonly the self-consistent calculations of the DFT or Hartree-Fock for nuclear structure do not consider this difference, it is known that the finite-size effect of protons is not negligible in the study of isobaric analog energy [4]. One more essential point is that it is difficult to consider the form factor of protons for the finite-size effect in the exact-Fock term as the single-particle wave functions are used. In contrast, one is able to consider this effect in the PBE-GGA Coulomb exchange functional since the functional is written only in terms of the density.

A more challenging topic is a Coulomb correlation EDF for nuclear systems. In electron systems, Coulomb correlation EDFs have been discussed for decades. However, these functionals are not applicable to nuclear systems [22]. This is because the correlation energy in nuclear systems is mainly caused by attractive nuclear interaction, whereas that in electron systems is mainly caused by repulsive Coulomb interaction, and thus, the Coulomb correlation energy in nuclear systems is opposite sign to the that in electron systems [22, 39, 40]. Therefore, to investigate the Coulomb correlation EDFs for nuclear systems is a very important topic in nuclear systems in the future.

ACKNOWLEDGMENTS

The authors appreciate Ryosuke Akashi, Shinji Tsuneyuki, and Enrico Vigezzi for stimulating discussions and valuable comments. TN and HL would like to thank the RIKEN iTHEMS program, and the JSPS-NSFC Bilateral Program for Joint Research Project on Nuclear mass and life for unraveling mysteries of the r-process. TN acknowledges the financial support from Computational Science Alliance, the University of Tokyo. HL acknowledges the JSPS Grant-in-Aid for Early-Career Scientists under Grant No. 18K13549. GC and XRM acknowledge funding from the European Union's Horizon 2020 research and innovation program under Grant No. 654002.

Appendix A: Potential and rearrangement term in generalized gradient approximation

In the self-consistent calculation, a potential form of the Coulomb exchange functional is required. Since the LDA Coulomb exchange functional is

$$E_{\text{Cx}}^{\text{LDA}}[\rho] = -\frac{3}{4} \frac{e^2}{4\pi\epsilon_0} \left(\frac{3}{\pi}\right)^{1/3} \int [\rho(\mathbf{r})]^{4/3} d\mathbf{r}, \quad (\text{A1})$$

the LDA Coulomb exchange potential is

$$\begin{aligned} V_{\text{Cx}}^{\text{LDA}}(\mathbf{r}) &= \frac{\delta E_{\text{Cx}}^{\text{LDA}}[\rho(\mathbf{r})]}{\delta \rho(\mathbf{r})} \\ &= \varepsilon_{\text{Cx}}^{\text{LDA}}(\rho) + \rho(\mathbf{r}) \frac{\partial \varepsilon_{\text{Cx}}^{\text{LDA}}(\rho)}{\partial \rho} \\ &= -\frac{e^2}{4\pi\epsilon_0} \left(\frac{3}{\pi}\right)^{1/3} [\rho(\mathbf{r})]^{1/3}, \end{aligned} \quad (\text{A2})$$

where $\varepsilon_{\text{Cx}}^{\text{LDA}}$ is the exchange energy density

$$\varepsilon_{\text{Cx}}^{\text{LDA}}(\rho) = -\frac{3}{4} \frac{e^2}{4\pi\epsilon_0} \left(\frac{3}{\pi}\right)^{1/3} \rho^{1/3}. \quad (\text{A3})$$

In order to go beyond the LDA, the GGA Coulomb exchange functional and energy density are

$$E_{\text{Cx}}^{\text{GGA}}[\rho] = -\frac{3}{4} \frac{e^2}{4\pi\epsilon_0} \left(\frac{3}{\pi}\right)^{1/3} \int [\rho(\mathbf{r})]^{4/3} F(s(\mathbf{r})) d\mathbf{r}, \quad (\text{A4})$$

$$\varepsilon_{\text{Cx}}^{\text{GGA}}(\rho) = -\frac{3}{4} \frac{e^2}{4\pi\epsilon_0} \left(\frac{3}{\pi}\right)^{1/3} \rho^{1/3} F(s), \quad (\text{A5})$$

respectively. Thus, the GGA Coulomb exchange potential is [41]

$$\begin{aligned} V_{\text{Cx}}^{\text{GGA}}(\mathbf{r}) &= \frac{\delta E_{\text{Cx}}^{\text{GGA}}[\rho(\mathbf{r})]}{\delta \rho(\mathbf{r})} \\ &= \varepsilon_{\text{Cx}}^{\text{GGA}}(\rho) + \rho \frac{\partial \varepsilon_{\text{Cx}}^{\text{GGA}}(\rho)}{\partial \rho} - \nabla \cdot \left(\rho \frac{\partial \varepsilon_{\text{Cx}}^{\text{GGA}}(\rho)}{\partial \nabla \rho} \right) \\ &= V_{\text{Cx}}^{\text{LDA}}(\mathbf{r}) F(s(\mathbf{r})) \\ &\quad + \varepsilon_{\text{Cx}}^{\text{LDA}}(\rho) \left(\frac{\nabla \rho \cdot \nabla |\nabla \rho|}{2k_{\text{F}} |\nabla \rho|^2} - \frac{4}{3}s - \frac{1}{2k_{\text{F}} |\nabla \rho|} \right) \frac{dF(s)}{ds} \\ &\quad - \varepsilon_{\text{Cx}}^{\text{LDA}}(\rho) \left(\frac{\nabla \rho \cdot \nabla |\nabla \rho|}{(2k_{\text{F}})^2 \rho |\nabla \rho|} - \frac{4}{3}s^2 \right) \frac{d^2 F(s)}{ds^2}, \end{aligned} \quad (\text{A6})$$

where the enhancement factors F for the PBE-GGA Coulomb exchange functional [25] for $\lambda = 1.00, 1.25,$ and 1.50 as functions of s are shown in dot-dashed, solid, and dashed lines, respectively, in Fig. 6. The GGA Coulomb exchange potential shown in Eq. (A6) is applicable for general GGA Coulomb exchange functionals, including the PBE-GGA Coulomb exchange functionals. Under the spherical symmetry, Eq. (A6) is simplified as

$$V_{\text{Cx}}^{\text{GGA}}(r) = V_{\text{Cx}}^{\text{LDA}}(r) \left[F(s(r)) - \left(s + \frac{3}{4} \frac{1}{k_{\text{F}} r} \right) \frac{dF}{ds} + \left(s^2 - \frac{3}{4} \frac{\rho''}{4\rho k_{\text{F}}} \right) \frac{d^2 F}{ds^2} \right], \quad (\text{A7})$$

where $\rho'' = d^2\rho(r)/dr^2$.

Next, the total energy is considered. On the one hand, in the original DFT, the total energy is written as [23]

$$E_{\text{gs}} = \sum_j \varepsilon_j + E_{\text{xc}}[\rho_{\text{gs}}] - \int V_{\text{xc}}(\mathbf{r}) \rho_{\text{gs}}(\mathbf{r}) d\mathbf{r} + \frac{1}{2} \iint V_{\text{int}}(\mathbf{r}, \mathbf{r}') \rho_{\text{gs}}(\mathbf{r}) \rho_{\text{gs}}(\mathbf{r}') d\mathbf{r} d\mathbf{r}', \quad (\text{A8})$$

where V_{int} is the two-body interaction, E_{xc} is the exchange-correlation functional, which shows the exchange energy and the remaining part of the total energy, and V_{xc} is the exchange-correlation potential defined as $V_{\text{xc}} = \delta E_{\text{xc}}/\delta\rho|_{\rho=\rho_{\text{gs}}}$. On the other hand, in the Skyrme Hartree-Fock calculation, the total energy reads

$$E_{\text{gs}} = \frac{1}{2} \sum_j (\varepsilon_j + \tau_j) + E_{\text{rea}}, \quad (\text{A9})$$

where ε_j and τ_j are the single-particle energy and the single-particle kinetic energy, respectively, and E_{rea} is the energy of rearrangement term [32]. Two expressions for the total energy Eqs. (A8) and (A9) should be identical to each other. Since the single-particle Kohn-Sham Hamiltonian is

$$\hat{h} = \hat{t} + V_{\text{xc}}(\mathbf{r}) + \int V_{\text{int}}(\mathbf{r}, \mathbf{r}') \rho_{\text{gs}}(\mathbf{r}') d\mathbf{r}', \quad (\text{A10})$$

where \hat{t} is the single-particle kinetic operator, the equation

$$\sum_j (\varepsilon_j - \tau_j) = \int V_{\text{xc}}(\mathbf{r}) \rho_{\text{gs}}(\mathbf{r}) d\mathbf{r} + \iint V_{\text{int}}(\mathbf{r}, \mathbf{r}') \rho_{\text{gs}}(\mathbf{r}) \rho_{\text{gs}}(\mathbf{r}') d\mathbf{r} d\mathbf{r}' \quad (\text{A11})$$

follows, and therefore Eq. (A8) reads

$$E_{\text{gs}} = \frac{1}{2} \sum_j (\varepsilon_j + \tau_j) + E_{\text{xc}}[\rho_{\text{gs}}] - \frac{1}{2} \int V_{\text{xc}}(\mathbf{r}) \rho_{\text{gs}}(\mathbf{r}) d\mathbf{r}. \quad (\text{A12})$$

As compared to Eq. (A9), the rearrangement term is

$$E_{\text{rea}} = E_{\text{xc}}[\rho_{\text{gs}}] - \frac{1}{2} \int V_{\text{xc}}(\mathbf{r}) \rho_{\text{gs}}(\mathbf{r}) d\mathbf{r}. \quad (\text{A13})$$

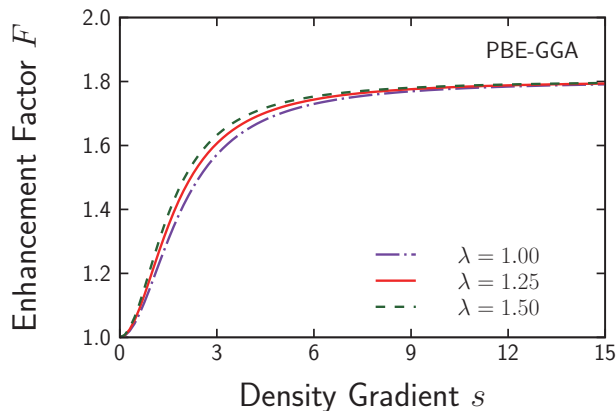


FIG. 6. Enhancement factors F for the PBE-GGA [25] for $\lambda = 1.00, 1.25,$ and 1.50 as functions of s shown in dot-dashed, solid, and dashed lines, respectively.

-
- [1] J. A. Nolen, Jr. and J. P. Schiffer, *Annu. Rev. Nucl. Sci.* **19**, 471 (1969).
- [2] J. Jänecke, *Nucl. Phys.* **73**, 97 (1965).
- [3] S. Shlomo, *Rep. Prog. Phys.* **41**, 957 (1978).
- [4] X. Roca-Maza, G. Colò, and H. Sagawa, *Phys. Rev. Lett.* **120**, 202501 (2018).
- [5] S. A. Coon and M. D. Scadron, *Phys. Rev. C* **26**, 2402 (1982).
- [6] H. Liang, N. Van Giai, and J. Meng, *Phys. Rev. C* **79**, 064316 (2009).
- [7] J. C. Hardy and I. S. Towner, *Phys. Rev. C* **91**, 025501 (2015).
- [8] C. Titin-Schnaider and P. Quentin, *Phys. Lett. B* **49**, 397 (1974).
- [9] M. Anguiano, J. Egidio, and L. Robledo, *Nucl. Phys. A* **683**, 227 (2001).
- [10] J. Skalski, *Phys. Rev. C* **63**, 024312 (2001).
- [11] J. Le Bloas, M.-H. Koh, P. Quentin, L. Bonneau, and J. I. A. Ithnin, *Phys. Rev. C* **84**, 014310 (2011).
- [12] X. Roca-Maza, L.-G. Cao, G. Colò, and H. Sagawa, *Phys. Rev. C* **94**, 044313 (2016).
- [13] W.-H. Long, N. Van Giai, and J. Meng, *Phys. Lett. B* **640**, 150 (2006).
- [14] H. Liang, N. Van Giai, and J. Meng, *Phys. Rev. Lett.* **101**, 122502 (2008).
- [15] P. A. M. Dirac, *Proc. Camb. Phil. Soc.* **26**, 376 (1930).
- [16] J. C. Slater, *Phys. Rev.* **81**, 385 (1951).

- [17] H.-Q. Gu, H. Liang, W. H. Long, N. Van Giai, and J. Meng, *Phys. Rev. C* **87**, 041301 (2013).
- [18] S.-H. Shen, J.-N. Hu, H.-Z. Liang, J. Meng, P. Ring, and S.-Q. Zhang, *Chin. Phys. Lett.* **33**, 102103 (2016).
- [19] S. Shen, H. Liang, J. Meng, P. Ring, and S. Zhang, *Phys. Rev. C* **96**, 014316 (2017).
- [20] M. Bender, P.-H. Heenen, and P.-G. Reinhard, *Rev. Mod. Phys.* **75**, 121 (2003).
- [21] H. Liang, J. Meng, and S.-G. Zhou, *Phys. Rep.* **570**, 1 (2015).
- [22] T. Naito, R. Akashi, and H. Liang, *Phys. Rev. C* **97**, 044319 (2018).
- [23] E. Engel and R. M. Dreizler, *Density Functional Theory—An Advanced Course*, Theoretical and Mathematical Physics (Springer-Verlag, Berlin, Heidelberg, 2011).
- [24] J. P. Perdew, K. Burke, and Y. Wang, *Phys. Rev. B* **54**, 16533 (1996).
- [25] J. P. Perdew, K. Burke, and M. Ernzerhof, *Phys. Rev. Lett.* **77**, 3865 (1996).
- [26] J. P. Perdew, A. Ruzsinszky, G. I. Csonka, O. A. Vydrov, G. E. Scuseria, L. A. Constantin, X. Zhou, and K. Burke, *Phys. Rev. Lett.* **100**, 136406 (2008).
- [27] J. P. Perdew, J. A. Chevary, S. H. Vosko, K. A. Jackson, M. R. Pederson, D. J. Singh, and C. Fiolhais, *Phys. Rev. B* **46**, 6671 (1992).
- [28] E. H. Lieb and S. Oxford, *Int. J. Quantum Chem.* **19**, 427 (1981).
- [29] E. H. Lieb and M. Loss, *Analysis*, 2nd ed., Graduate Studies in Mathematics (American Mathematical Society, Providence, Rhode Island, 2001).
- [30] M. Levy and J. P. Perdew, *Phys. Rev. A* **32**, 2010 (1985).
- [31] P. R. Antoniewicz and L. Kleinman, *Phys. Rev. B* **31**, 6779 (1985).
- [32] D. Vautherin and D. M. Brink, *Phys. Rev. C* **5**, 626 (1972).
- [33] X. Roca-Maza, G. Colò, and H. Sagawa, *Phys. Rev. C* **86**, 031306 (2012).
- [34] G. Colò, L. Cao, N. Van Giai, and L. Capelli, *Comput. Phys. Commun.* **184**, 142 (2013).
- [35] X. Roca-Maza and N. Paar, *Prog. Part. Nucl. Phys.* **101**, 96 (2018).
- [36] I. Angeli and K. Marinova, *At. Data Nucl. Data Tables* **99**, 69 (2013).
- [37] M.-C. Kim, E. Sim, and K. Burke, *Phys. Rev. Lett.* **111**, 073003 (2013).
- [38] P. J. Mohr, D. B. Newell, and B. N. Taylor, *Rev. Mod. Phys.* **88**, 035009 (2016).
- [39] A. Bulgac and V. R. Shaginyan, *Nucl. Phys. A* **601**, 103 (1996).
- [40] A. Bulgac and V. R. Shaginyan, *Phys. Lett. B* **469**, 1 (1999).
- [41] J. Carmona-Espíndola, J. L. Gázquez, A. Vela, and S. B. Trickey, *J. Chem. Phys.* **142**, 054105 (2015).